Preprints.org

Article

Not peer-reviewed version

Patient-Derived Free-Floating Non-Small Cell Lung Cancer Organoids: A Versatile Tool for Personalized Testing of Chemotherapeutic Drugs

Lilian Ismail , Komal Zahid , Anna Polyanskaya , Aya Al Othman , Ningfei Shen , Xiaoli Qi , Rushan A. Sulimanov , Yuri Esakov , Vladimir A. Makarov , Gleb I. Filkov , Alexander V. Trofimenko , Alexandre Mezentsev , Mikhail Durymanov *

Posted Date: 29 December 2023

doi: 10.20944/preprints202312.2280.v1

Keywords: Free-floating organoids; non-small cell lung cancer; cytokine; drug resistance; personalized medicine

Preprints.org is a free multidiscipline platform providing preprint service that is dedicated to making early versions of research outputs permanently available and citable. Preprints posted at Preprints.org appear in Web of Science, Crossref, Google Scholar, Scilit, Europe PMC.

Copyright: This is an open access article distributed under the Creative Commons Attribution License which permits unrestricted use, distribution, and reproduction in any medium, provided the original work is properly cited.

Preprints (www.preprints.org) | NOT PEER-REVIEWED | Posted: 29 December 2023 doi:10.20944/preprints202312.2280.v1

Disclaimer/Publisher's Note: The statements, opinions, and data contained in all publications are solely those of the individual author(s) and contributor(s) and not of MDPI and/or the editor(s). MDPI and/or the editor(s) disclaim responsibility for any injury to people or property resulting from any ideas, methods, instructions, or products referred to in the content.

Article

Patient-Derived Free-Floating Non-Small Cell Lung Cancer Organoids: A Versatile Tool for Personalized Testing of Chemotherapeutic Drugs

Lilian Ismail [a], Komal Zahid [a], Anna Polyanskaya [a], Aya Al Othman [a,b], Shen Ningfei [a,b], Xiaoli Qi [a,b], Rushan Sulimanov [b], Yuri Esakov [c], Vladimir Makarov [b], Gleb Filkov [a], Alexander Trofimenko [a], Alexandre Mezentsev [a,b] and Mikhail Durymanov [a,b,*]

[a] School of Biological and Medical Physics, Moscow Institute of Physics and Technology, Dolgoprudny, Moscow Region, Russia
[b] Medical Informatics Laboratory, Yaroslav-the-Wise Novgorod State University, Veliky Novgorod, Russia
[c] Moscow State Budgetary Healthcare Institution «Moscow City Oncological Hospital No. 1, Moscow Healthcare Department, Moscow, Russia

* Correspondence: author: Dr. Mikhail Durymanov, PhD, Associate Professor, Deputy Head of Special Cell Technology Lab, Moscow Institute of Physics and Technology (State University), Institutsky per. 9, Dolgoprudny, Moscow Region, 141701, Russian Federation, Phone: +7(977)371-17-58, e-mail: durymanov.mo@mipt.ru

Abstract: Patient-derived tumor organoids (PDTOs) are a novel preclinical model of non-small cell lung cancer (NSCLC) for studying tumor biology and precision medicine, which recapitulates tumor morphology and gene expression profile. However, some issues such as low establishment rates, long-term production, and the loss of the immune microenvironment have hindered their widespread practical use. In this study, we investigated the efficacy of a recently introduced free-floating organoid production method to address these issues. The free-floating approach provided PDTO establishment success rate of over 90 % resulting in organoid formation within a short period of one week. These organoids retained the elements of the parental tumor morphology and contained stroma and immune cell populations, as confirmed by flow cytometry analysis. Importantly, we found that the cytokine and growth factor expression profiles of the free-floating organoids correlated with those of the original tumors in 58 % of cases, indicating the preservation of tumor-associated signaling pathways. Obtained organoids exhibited different responses to anticancer chemotherapeutics that might be a result of variable expression of drug resistance-associated genes. Considering the high establishment rate and short time of free-floating organoid production, this technique provides a valuable tool for a more accurate evaluation of therapeutic strategies and cancer biology studies.

Keywords: free-floating organoids; non-small cell lung cancer; cytokine; drug resistance; personalized medicine

1. INTRODUCTION

In spite of significant advances in treatment modalities in the last decade, lung cancer remains the first-ranked contributor to cancer-related deaths worldwide.[1] Non-small cell lung cancer (NSCLC) with approximately 15-20 % 5-year survival rate[2] accounts for 80 % of all lung cancer cases.[1] Poor survival rate is partially attributed to the lack of an accurate prognostic method to evaluate treatment outcomes that would help to select a suitable experimentally-based treatment regimen for a certain patient. Although genomics and transcriptomics technologies have opened an avenue for precision medicine by linking genetic alterations and upregulated signaling pathways to targeted drugs,[3,4] there are no reliable biomarkers for prediction of tumor responses to chemotherapy,[5,6] which remains a major treatment option for advanced NSCLC.[7,8]

© 2023 by the author(s). Distributed under a Creative Commons CC BY license.

Preprints (www.preprints.org) | NOT PEER-REVIEWED | Posted: 29 December 2023 doi:10.20944/preprints202312.2280.v1

Two approaches have been developed to address this concern. First, patient-derived xenografts (PDXs) have been employed initially to assess drug responsiveness, but their efficacy has been hampered by low success rates, extended turnaround times, and substantial costs.[9] More recent alternative, patient-derived tumor organoids (PDTOs) and spheroids, have emerged as a robust and reliable *in vitro* model for precision medicine.[10] Increasing evidence confirms the phenotypic and genotypic correspondence between original tumor tissues and PDTOs across various cancers.[11–15] Some clinical studies have demonstrated the high prognostic value of PDTOs for evaluation of patient responses to therapies.[16,17] However, several challenges impede the clinical integration of PDTO-based drug sensitivity testing. Current PDTO-based tests often need weeks or months to yield results due to limited organoid quantities from patient samples and the use of conventional cell culture methods.[18] The success rate of establishing viable organoid cultures with steady expansion rates remains low for some tumor types.[19]

To date, there are two reported methods of organoid production. The first method is based on embedding of tumor-isolated cell microclusters in Matrigel™ domes and their further incubation in the medium encouraging growth of epithelial cells.[20] This submersion technique typically generates organoids composed solely of epithelial cells and does not incorporate any stromal or immune cells. The major limitation of this technique is loss of immune and stromal cells that can be critical for some applications, including study of checkpoint blockade mechanisms.[21] Another method is designed to produce PDTOs from micropieces of tumor tissue followed by their incorporation in collagen I gel and cultivation in air-liquid culture system.[22] Once this technique relies on mechanical disintegration of tumor tissue only, it seems to provide non-uniform organoids that can be an obstacle to personalized drug testing.

Here, we produced NSCLC PDTOs using a novel method, which has been tested earlier for generation of highly fibrotic and more drug-resistant NSCLC spheroids.[23] This technique exploits stimuli-responsive ECM-mimicking gel that allows to obtain free-floating organoids in a short time. The main goal of this study is to assess the efficacy of free-floating NSCLC PDTO production and to characterize them. In particular, we evaluated morphology, cell composition, cytokine and growth factor expression profile in NSCLC PDTO and found them to some extent consistent with the original tumors. Additionally, we demonstrated feasibility to perform testing of clinically recommended chemotherapeutic drugs using free-floating PDTOs within 1.5-weeks, avoiding the need for long-term culture. Thus, the use of free-floating organoids could be a promising tool for personalization of treatment options in NSCLC and understanding the mechanisms implicated in resistance to the certain drugs.

2. MATERIALS AND METHODS

2.1. Human specimens

Small tissue fragments of 1 cm^3 volume were obtained from surgically resected lung specimens of both lung tumor tissues and non-neoplastic tissues. Informed consent was obtained from all patients prior to tissue acquisition, and they were informed of the potential risks and benefits of participating in the study. The research plan received approval from the Ethics Committee of the City Clinical Oncological Hospital No. 1 (Moscow, Russia), and all procedures were conducted in accordance with all relevant national and international regulations regarding the ethical use of human subjects. Histopathological examination definitively identified samples as either tumor or normal tissue. Expert pathologists confirmed the diagnosis for each case.

2.2. Free-floating organoid generation

Upon surgical resection, lung tumor tissues were immersed in DMEM/F12 (Gibco) growth medium containing 1 % PenStrep (PanEco, Moscow, Russia) and promptly transported to the laboratory on ice within 12 hours. Next, the tumor tissues were sectioned into multiple pieces. One piece was embedded in HistoPrep tissue embedding media (Fisher Scientific, Ottawa, Canada), and kept frozen at -80°C for further immunostaining. A second piece was preserved in RNeasy solution

Preprints (www.preprints.org) | NOT PEER-REVIEWED | Posted: 29 December 2023 doi:10.20944/preprints202312.2280.v1

(Evrogen, Moscow, Russia) to enable subsequent total RNA isolation. A third piece was fixed in 10 % buffered formalin (Thermo Fisher Scientific) for H&E staining. Another piece was used for preparation of tissue lysate for immunoblotting. The remaining tissue was finely minced using surgical scissors and suspended in 10 mL of DMEM/F12 growth medium containing 1 % PenStrep and 1 mg mL^{-1} collagenase I (Gibco). Upon 1.5-hour incubation at 37°C with slow and gentle agitation, the digested tissue suspension was passed through a 70-μm cell strainer (Falcon). The obtained cell suspension was centrifuged at 1,500 rpm for 5 min at 18-20°C, followed by the pellet washing with HBSS and resuspension in 6 mL of fresh growth medium for organoids (DMEM/F12 supplemented with 20 ng mL^{-1} bFGF (10014-HNAE, SinoBiological, China), 50 ng mL^{-1} human EGF (ab55566, Abcam), N2 (PanEco, Moscow, Russia), NeuroMax (PanEco, Moscow, Russia), 10 mM Glutamax (Gibco), 1 mM N-acetyl cysteine (Sigma), 10 mM nicotinamide (Sigma), 10 μM Y27631 (ab120129, Abcam), 15 μM HEPES (Sigma) and 1 % PenStrep). The cells were counted using a hemocytometer. A part of collected cells was frozen for further flow cytometry analysis.

To produce free-floating NSCLC organoids, 96-well plates were initially coated with 50 μL of a 1 % w/v agarose solution in Milli-Q water. This coating was allowed to solidify at room temperature for approximately 20-30 min. Subsequently, a collagen-based gel solution with resuspended tumor cells was prepared using SANATO 3D culture gel kit (#FTBM0051, Phystech Biomed, Russia) and 1 % (v/v) SANATO reagent (#FTBM0050, Phystech Biomed, Russia) according to manufacturer's protocol. Subsequently, 25 μL gel domes containing 50,000 cells were dispensed into each well, and the gel was allowed to solidify at 37°C for 20 min. After gelation, 100 μL of growth medium for organoids was added to each well, and the plates were placed in an incubator, where they were cultured at 37°C in humidified atmosphere containing 5 % CO_2. Growth medium was changed every other day during all time of the experiment. The organoids were subjected to daily examination for a period of 14 days, during which their size and morphology were observed using bright field microscopy with an AxioVert.A1 microscope (Zeiss, Oberkochen, Germany). Organoid areas were determined in the brightfield images using ImageJ software (1.42v, US National Institutes of Health, USA).

2.3. Histological analysis

Collected tumor tissues and 2-week-old free-floating PDTOs were incubated for 5 days in 10 % buffered neutral formalin (Thermo Fisher Scientific), embedded in paraffin wax, and cut into 5-μm thickness slices, followed by staining with hematoxylin-eosin. The sections have been photographed using an inverted Olympus CX41 (Olympus Co., Tokyo, Japan) equipped with a UPlanApo 20×/NA 0.70 objective lens.

2.4. Immunohistochemistry analysis

One-week-old free-floating NSCLC PDTOs were harvested, embedded into HistoPrep tissue embedding media (Fisher Scientific, Ottawa, Canada), and frozen at −20°C. Subsequently, the frozen blocks with organoids and original tumor tissues were cut into 10-μm thickness sections, fixed in the mixture of acetone and methanol (1:1) for 15 min, and air-dried at room temperature. To identify the desired ECM proteins, the slides were washed with TBS-T (1x) and kept in blocking solution for 1 h at room temperature. Then, samples were incubated with primary antibodies for 3 h at room temperature. To stain ECM components rabbit monoclonal anti-fibronectin primary antibodies (ab2413, Abcam), rabbit polyclonal anti-type I collagen antibodies (ab34710, Abcam), and rabbit polyclonal anti-laminin antibodies (ab11575, Abcam) were used. After incubation with primary antibodies, the samples were washed with TBS-T and incubated with goat anti-rabbit IgG labeled with Alexa Fluor 488 (ab150077, Abcam) for 1 h at room temperature. Nuclear DNA was stained with DAPI for 10 min before the samples were covered with a cover glass. The images of tumor tissue and organoid sections were obtained using an inverted AxioVert.A1 microscope (Zeiss, Oberkochen, Germany) equipped with ×20/0.6 objective lens.

2.5. Western blotting

Preprints (www.preprints.org) | NOT PEER-REVIEWED | Posted: 29 December 2023 doi:10.20944/preprints202312.2280.v1

NSCLC PDTO or tumor tissue lysates containing equal amounts of total protein (15 μg) were mixed with loading buffer, boiled for 5 min, separated by denaturing 12.5 % SDS-polyacrylamide gel and transferred to Amersham™ Hybond™ 0.45 μm PVDF membrane (GE Healthcare, UK). The membrane was blocked for 1 h with a blocking buffer (Bio-Rad) under gentle agitation and incubated overnight with antibodies against thyroid transcription factor TTF1 (ab76013, Abcam) for adenocarcinomas, p63 (ab247245, Abcam) for squamous cell carcinomas, or β-actin (ab8227, Abcam) as a reference. Then, the membrane was washed twice with TBS-T and incubated with HRP conjugated secondary antibody (ab205718, Abcam) at room temperature for 1 h, followed by several washings with TBS-T and deionized water. Protein bands were visualized by ChemiDoc XRS+ imaging system (Bio-Rad, Hercules, CA) using chemiluminescence mode. The signal intensities were normalized to β-actin. The quantification was performed using Quantity One software (Bio-Rad, Hercules, CA, USA).

2.6. Flow cytometry

One-week-old NSCLC PDTOs were collected and treated with 1 % collagenase I for 0.5-1 h at 37°C. The cells, isolated from disintegrated organoids, were washed with ice-cold Versene solution and used for sample preparation. Unfrozen cells, isolated earlier from the parental tumors, were also washed with ice-cold Versene solution and processed for sample preparation. Three samples were stained with antibodies against surface markers CD206 (ab195192, Abcam), PD-L1 (ab205921, Abcam), and CD8 (ab17147, Abcam) to determine M2-polarized tumor-associated macrophages, cancer cells, and T-killer cells, respectively. The samples, stained with anti-PD-L1 and anti-CD8 IgGs, were also treated with fluorescently labeled secondary antibodies (ab150113 and ab150115, Abcam). Another sample was fixed in 4 % paraformaldehyde with 0.1 % Triton X-100, followed by staining with antibodies against α-smooth muscle actin (α-SMA) (ab124964, Abcam) to determine myofibroblasts and secondary antibodies (ab150113, Abcam). The staining was carried out at 1:100 and 1:200 antibody dilutions for the primary and secondary antibodies, respectively. To minimize non-specific IgG binding, the cell staining was performed in 1 % BSA and 10 % FBS solution. Unbound antibodies were removed by washing with PBS. Recommended isotype controls were used as negative controls to exclude non-specific binding events. The cells were subjected to flow cytometry analysis using CytoFLEX flow cytometer (Beckman Coulter, Brea, CA). Per sample, 10,000 events were gated.

2.7. RNA extraction and qRT-PCR

Total RNA was isolated using ExtractRNA kit (Evrogen, Moscow, Russia) in accordance with the manufacturer's protocol. The prepared samples were subjected to spectral analysis. If the absorption ratio A260/A280 was lower than 2.0, the samples were purified again using CleanRNA Standard (Evrogen, Moscow, Russia). cDNA was synthesized by random priming from 1 μg of total RNA using the MMLV RT kit (Evrogen, Moscow, Russia). These samples were subjected to qPCR using CFX96 Real-Time PCR Detection System (Bio-Rad, Hercules, CA, USA) with the primers listed in Supplemental Table S1. For each reverse-transcribed sample, amplification of 18S rRNA served as an internal quantification standard. The results were analyzed using CFX Manager software supplied by the manufacturer. All samples were run in triplicate.

2.8. Cell viability assay

Viability of NSCLC tumor organoids treated or non-treated with anti-cancer drugs was assessed using CellTiter-Glo® 3D Cell Viability Assay (Promega, Madison, WI) according to the manufacturers' protocol. Briefly, the organoids were exposed to different concentrations of cisplatin, etoposide, pemetrexed, paclitaxel or gemcitabine (all from Sigma, St. Louis, MO) for 96 hours. Incubation of the organoids with drugs was carried out from day 7 to day 11. The final concentration of the drugs in wells was ranged from 0 to 2 μM. After incubation with drugs, equal volume of CellTiter-Glo® 3D reagent was added to the wells. Next, the plate was vigorously agitated for 5 min

Preprints (www.preprints.org) | NOT PEER-REVIEWED | Posted: 29 December 2023 doi:10.20944/preprints202312.2280.v1

and incubated for additional 25 min at room temperature in the dark. The luminescence was measured using microplate reader CLARIOstar Plus (BMG LABTECH, Ortenberg, Germany).

2.9. Statistical analysis

The statistical data analysis was carried out using Graphpad Prism 5 (GraphPad Software Inc., San Diego, CA) software. The data are presented as mean ± standard deviation (SD). Each experiment was performed as minimum in triplicate. To determine the statistical significance of the differences between two groups, the nonparametric Mann-Whitney U-test was performed. The value $p < 0.05$ was considered to indicate a statistically significant difference.

3. RESULTS

3.1. Characterization of free-floating NSCLC organoid morphology

The generation procedure of free-floating organoids resembles the conventional technique of PDTO production (Figure 1A). Similarly, the isolated tumor cells are placed into ECM-mimicking hydrogel, followed by incubation at standard conditions. At the same time, gradual shrinkage of stimuli-responsive gel in the used technique encourages cell-to-cell connections and rapid formation of multicellular aggregations, which are becoming free-floating organoids over time (Figure 1B).

We obtained free-floating PDTOs from different types of NSCLC tumors including adenocarcinoma, large-cell carcinoma, and squamous cell carcinoma (SCC) (Supplemental Figure S1A and Supplemental Table S2). The usage of this technique allowed us to obtain free-floating organoids with over 90 % probability (Supplemental Figure S1B). These organoids assembled within one week and had size over 200 microns (Figure 1C and D). Histological analysis of the obtained organoids confirmed their morphological integrity (Figure 1E), while immunoblotting analysis indicated the retention of adenocarcinoma- or SCC-specific markers TTF1 and p63, respectively (Figure 1F).

For further understanding of free-floating organoid tissue integrity, we examined the expression of extracellular (ECM) components. Immunohistochemistry analysis has shown that similar to the parental tumors, free-floating PDTOs produce stromal ECM proteins such as collagen I, and basement membrane-specific proteins including fibronectin and laminin (Figure 1G). As a part of tumor microenvironment, ECM can significantly contribute to enhanced chemoresistance by acting as a steric barrier to the diffusion of therapeutic agents[24] and by promoting pro-survival signaling.[10]

Preprints (www.preprints.org) | NOT PEER-REVIEWED | Posted: 29 December 2023 doi:10.20944/preprints202312.2280.v1

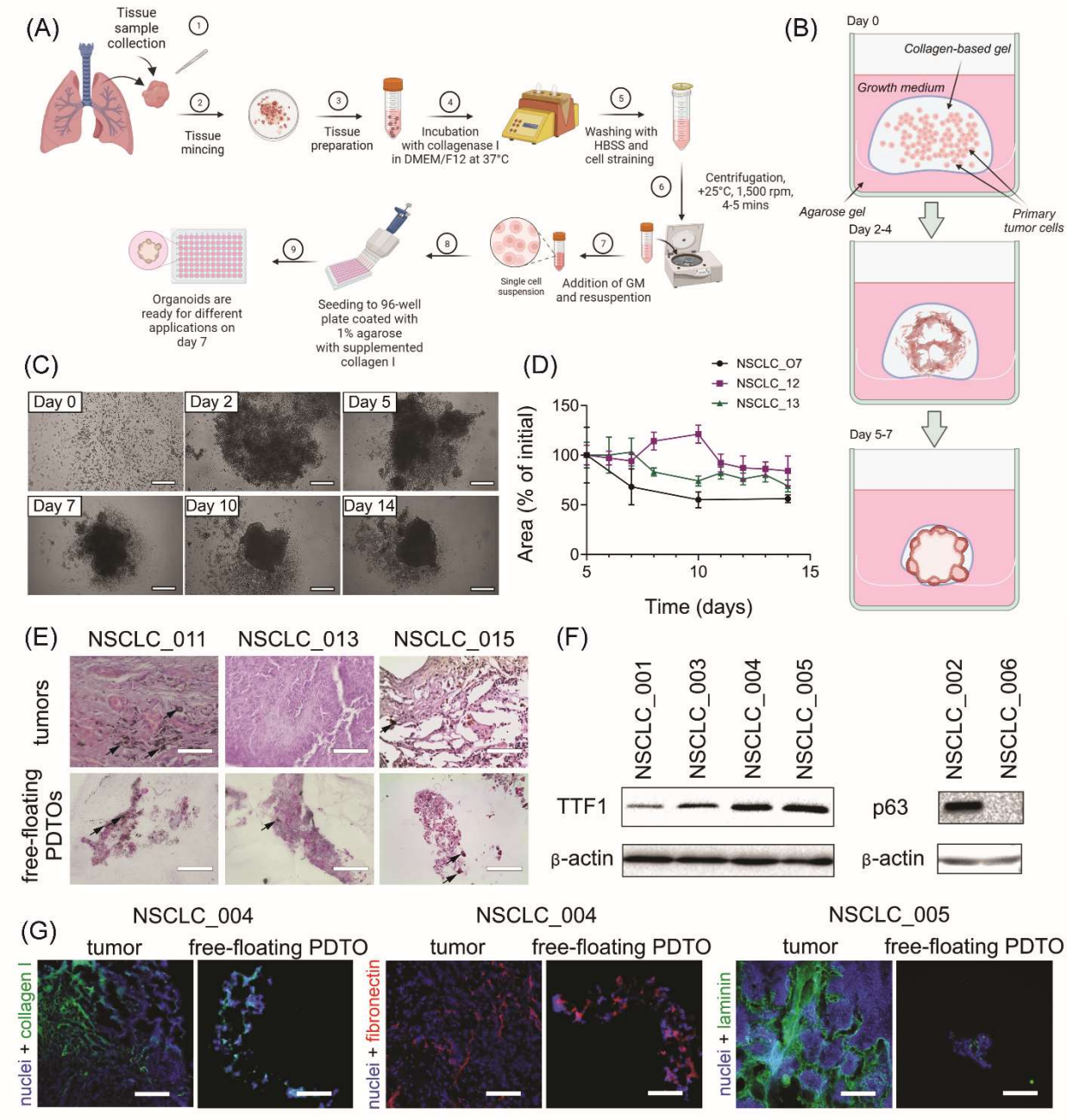

Figure 1. Production and characterization of free-floating NSCLC PDTOs. (A) The scheme of free-floating PDTO production. (B) The main stages of morphological changes in the obtained free-floating organoids. (C) Time-lapse monitoring of organoid morphological changes in transmitted light. The scale bar is 200 μm. (D) Kinetics of PDTO area change over time for NSCLC_007, NSCLC_012, NSCLC_013, measured using brightfield images. (E) Representative images of H&E stained histological sections of adenocarcinoma tumors and corresponding free-floating organoids from adenocarcinoma patients NSCLC_011, NSCLC_013, and NSCLC_015. Black arrows define soot deposits in the tissues and PDTOs of the smoker patients. The scale bar is 200 μm. (F) Immunoblotting analysis indicated the presence of lung adenocarcinoma-specific marker TTF1 and squamous-cell carcinoma-specific marker p63 (and its absence in large-cell carcinoma NSCLC_006) in the organoids obtained from the corresponding NSCLC tumors. (G) IHC analysis of ECM distribution in NSCLC tumors and organoids. Collagen I (green), fibronectin (red), and laminin (green) were detected in both tumors and free-floating PDTOs. DAPI staining indicates cell nuclei (blue). The scale bar is 200 μm.

3.2. Cell composition of free-floating NSCLC PDTOs

Preprints (www.preprints.org) | NOT PEER-REVIEWED | Posted: 29 December 2023 doi:10.20944/preprints202312.2280.v1

The most commonly used method of PDTO production results in organoids without immune and stromal cells that can be critical for mimicking immune microenvironment. To assess cell composition of free-floating PDTOs, we performed flow cytometry analysis. For cell phenotyping, we used four cell-specific markers (Figure 2A). First, we determined a percentage of cells expressing CD206, a marker of M2 tumor-associated macrophages.[25] Next, we defined the enrichment of the patient tumors and PDTOs with CD8+ T-cells and myofibroblasts expressing α-smooth muscle actin (αSMA). Finally, we also evaluated PD-L1-positive cell fraction. In tumor microenvironment, PD-L1 can be expressed by cancer cells and immune cells,[26] and its expression level is considered by some authors as a prognostic marker in NSCLC.[27–29]

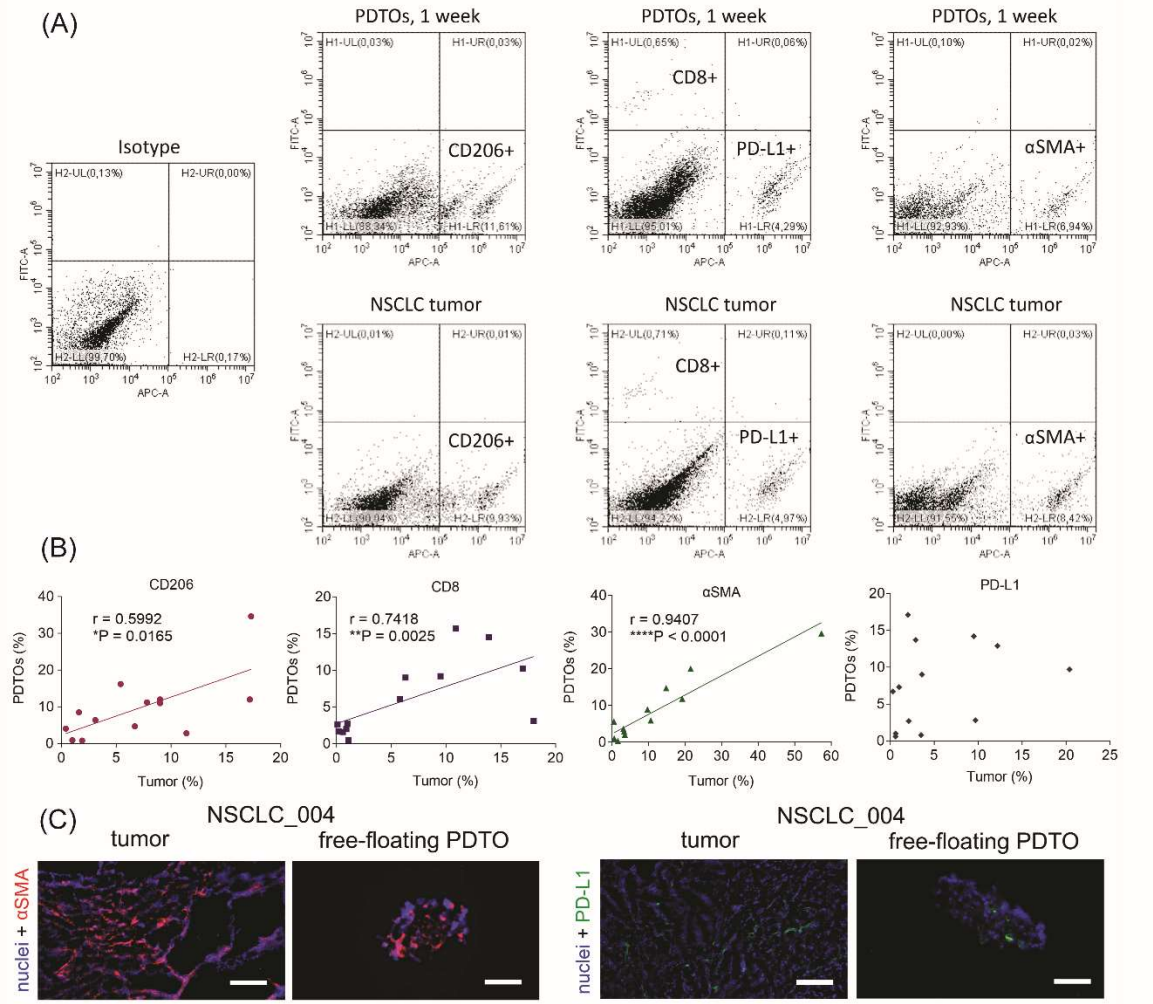

Figure 2. Cell composition of free-floating NSCLC PDTOs. (A) Gating of CD206+, PD-L1+, αSMA+, and CD8+ cells, isolated from original tumors or PDTOs. (B) Spearman correlations between cell compositions of PDTOs and parental tumors. Spearman's correlation coefficients and P-values were determined. (C) IHC images of αSMA+ (red) and PD-L1+ (green) cells in NSCLC tumors and free-floating organoids. DAPI staining indicates cell nuclei (blue). The scale bar is 200 μm.

It was found that free-floating PDTOs retain immune and stromal cells. Moreover, percentages of CD8+, CD206+, and αSMA + cells correlated between organoids and the original tumors (Figure 2B). IHC staining of tumor and organoid sections also confirmed the presence of αSMA+ and PD-L1+ in both specimens (Figure 2C). Thus, obtained results display the similarity of cell compositions between free-floating organoids and parental tumors.

3.3. Comparison of cytokine and growth factor expression profiles in PDTOs and parental tumors

Preprints (www.preprints.org) | NOT PEER-REVIEWED | Posted: 29 December 2023 doi:10.20944/preprints202312.2280.v1

The levels of 12 genes encoding cytokines and growth factors (*IFNG*, *TNFA*, *IL6*, *IL1B*, *IL12A*, *IL23A*, *IL10*, *TGFB*, *EGF*, *VEGFA*, *TSG6*, and *FGF2*), which play a significant role in NSCLC tumor microenvironment, were assessed within the tumor tissue as well as in the corresponding organoids. The RT-PCR analysis demonstrated remarkable variations in the gene expression profiles of cytokines/growth factors across NSCLC patients and free-floating organoids derived from them (Figure 3A). Considering separate samples, the expression profile correlated between free-floating PDTOs and the original tumors in 7 of 12 patients indicating a high extent of immune microenvironment mimicking in 3D culture (Figure 3A and Supplemental Table S3).

Considering separate cytokines and growth factors, the correlations in gene expression between tumors and organoids were found for six specific genes including *EGF*, *VEGFA*, *IL1B*, *IFNG*, *TNFA*, and *FGF2* (Figure 3B and Supplemental Table S4). These cytokines and growth factors significantly contribute to NSCLC progression and can be produced by various cell types in the tumor microenvironment, including cancer cells, fibroblasts, and immune cells.[30] For instance, EGF binds to and activates the EGFR receptor, which is associated with NSCLC tumor growth and increased survival rate.[31] FGF2 and VEGFA are both growth factors, which contribute to tumor angiogenesis.[32,33] TNFα and its receptor is a prognostic biomarker for NSCLC, which is associated with increased drug resistance and poor outcome.[34] IL-1β, a proinflammatory cytokine from the IL-1 family, contributes promoting tumor cell proliferation, pro-survival signaling, migration, and chemoresistance in NSCLC.[35] Finally, another proinflammatory cytokine IFNγ activates STAT1 transcription factor in lung adenocarcinoma cells that leads to PD-L1 upregulation and acquirement immune tolerance.[36] Thus, reproducing of cytokine/growth factor expression profile in free-floating organoids might be important for their use in the tumor-immune cell crosstalk studies.

Preprints (www.preprints.org) | NOT PEER-REVIEWED | Posted: 29 December 2023 doi:10.20944/preprints202312.2280.v1

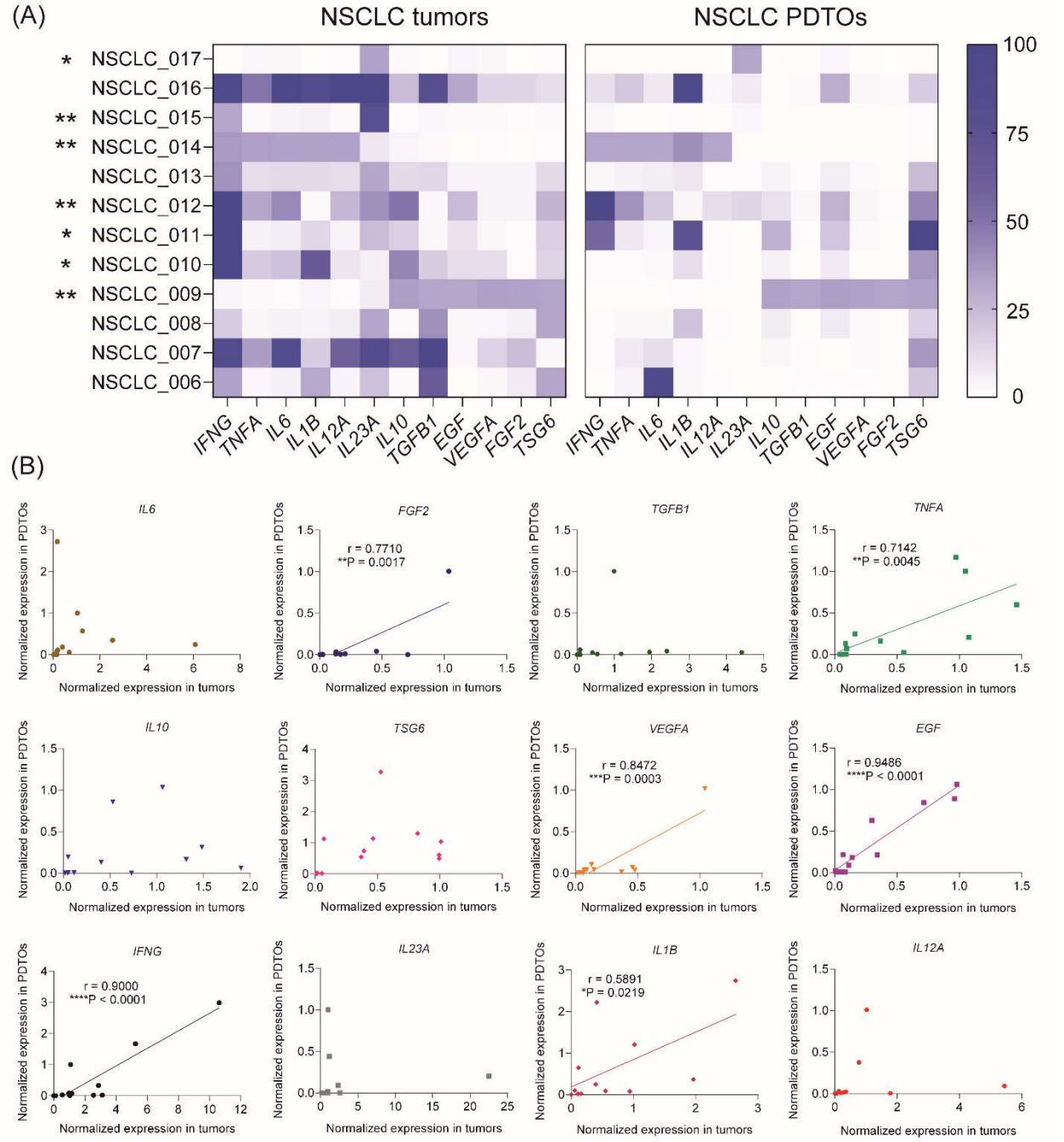

Figure 3. Gene expression profiles of cytokine and growth factor expression in the free-floating NSCLC PDTOs and parental tumors. (A) Heatmaps of normalized cytokine and growth factor gene expression profiles in NSCLC tumors and organoids. Spearman correlation analysis revealed statistically significant correlations between tumors and free-floating PDTOs in 7 of 12 samples (*P<0.05, **P<0.01) (see also Supplemental Table S3). (B) Spearman correlations between cytokine/growth factor expression in PDTOs and parental tumors. Spearman's correlation coefficients and P-values were determined for each gene (see also Supplemental Table S4).

3.4. Anticancer drug response of free-floating NSCLC PDTOs

To demonstrate feasibility of using free-floating NSCLC organoids for personalized drug sensitivity analysis, we evaluated their viability after exposure to five most commonly used chemotherapeutics including cisplatin, etoposide, pemetrexed, paclitaxel, and gemcitabine.

Preprints (www.preprints.org) | NOT PEER-REVIEWED | Posted: 29 December 2023 doi:10.20944/preprints202312.2280.v1

Noteworthy, the process of organoid generation and viability assay after drug exposure takes ten days that can be considered as a clinically relevant term.

Analysis of drug sensitivity indicates a broad diversity in IC50 values for different drugs across free-floating PDTOs from ten patients (Figure 4A and B). In some cases, IC50 values of PDTOs exceeded C_{max} values[37] for some drugs indicating these organoids to be resistance to the certain drugs (Supplemental Figure S2). Interestingly, free-floating organoids sometimes demonstrated a relatively high sensitivity to all drugs, like NSCLC_008, NSCLC_009, NSCLC_010, and NSCLC_011. However, in most cases the organoids exhibited drug resistance at least to one drug. Importantly, there were no cases of PDTO drug resistance to all drugs.

In this regard, *in vitro* patient-derived tumor models can be a valuable tool for personalized assessment of chemotherapeutic efficacy.

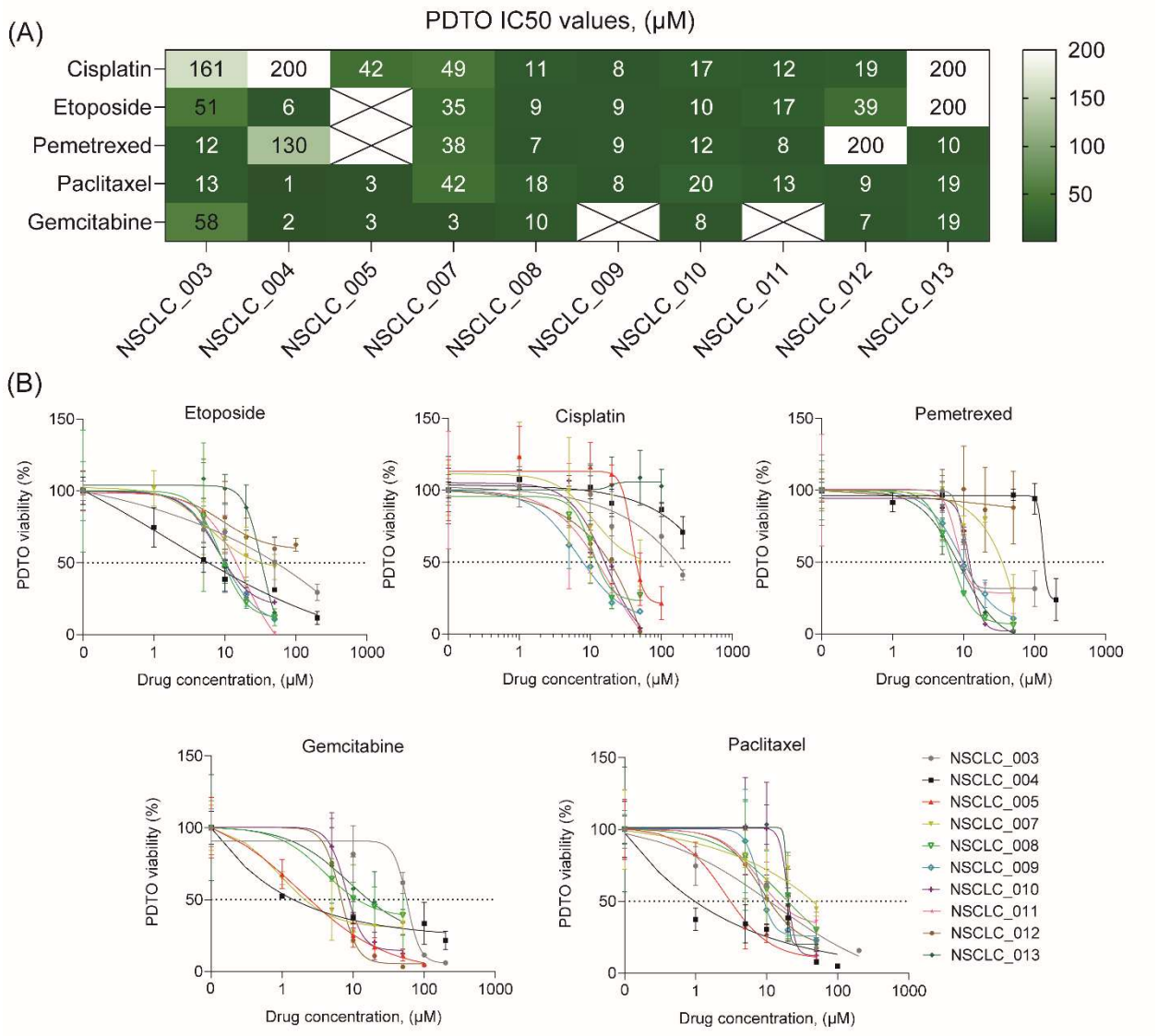

Figure 4. Drug sensitivity profiling of free-floating NSCLC PDTOs. (A) Heatmap of cisplatin, paclitaxel, gemcitabine, etoposide, and pemetrexed IC50 concentrations, determined for free-floating PDTOs from ten NSCLC patients. (B) Drug dose-dependent survival curves for free-floating PDTOs from ten NSCLC patients (see also Supplemental Figure S2).

3.5. Analysis of PDTO drug resistance

To understand a possible cause of drug response variation, we measured the mRNA expression levels of cytochrome P450 (CYP) and ATP-binding cassette (ABC) transporters, which can mediate drug resistance. Some CYPs make anticancer drugs more soluble and less toxic by oxydizing them,[38]

Preprints (www.preprints.org) | NOT PEER-REVIEWED | Posted: 29 December 2023 doi:10.20944/preprints202312.2280.v1

while transporters actively pump chemotherapy drugs out of cancer cells, thereby reducing their efficacy.[39]

PCR analysis demonstrated a high similarity in *CYP* expression levels between PDTOs and the original tumors (Figure 5A). At the same time, we did not find any trends in expression of different CYPs and resistance to certain drugs (Figure 5B). As for ABC transporter expression, we found some interesting points (Figure 5C). For instance, NSCLC_012 organoids with the highest *ABCC5* expression are resistant to pemetrexed. Indeed, ABCC5 was shown to mediate the inherited resistance to pemetrexed in several cancers.[40–42] According to our data, NSCLC_003 organoids with the highest *ABCG2* expression are more resistant to cisplatin. These data are in compliance with the results of previous studies demonstrating resistance of different tumors, including NSCLC, to this drug.[43–47] Interestingly, we observed very high variation in *CYP* and *ABC* expression across NSCLC PDTOs from different patients (Figure 5B and C) that probably shapes an individual resistance to chemotherapeutics.

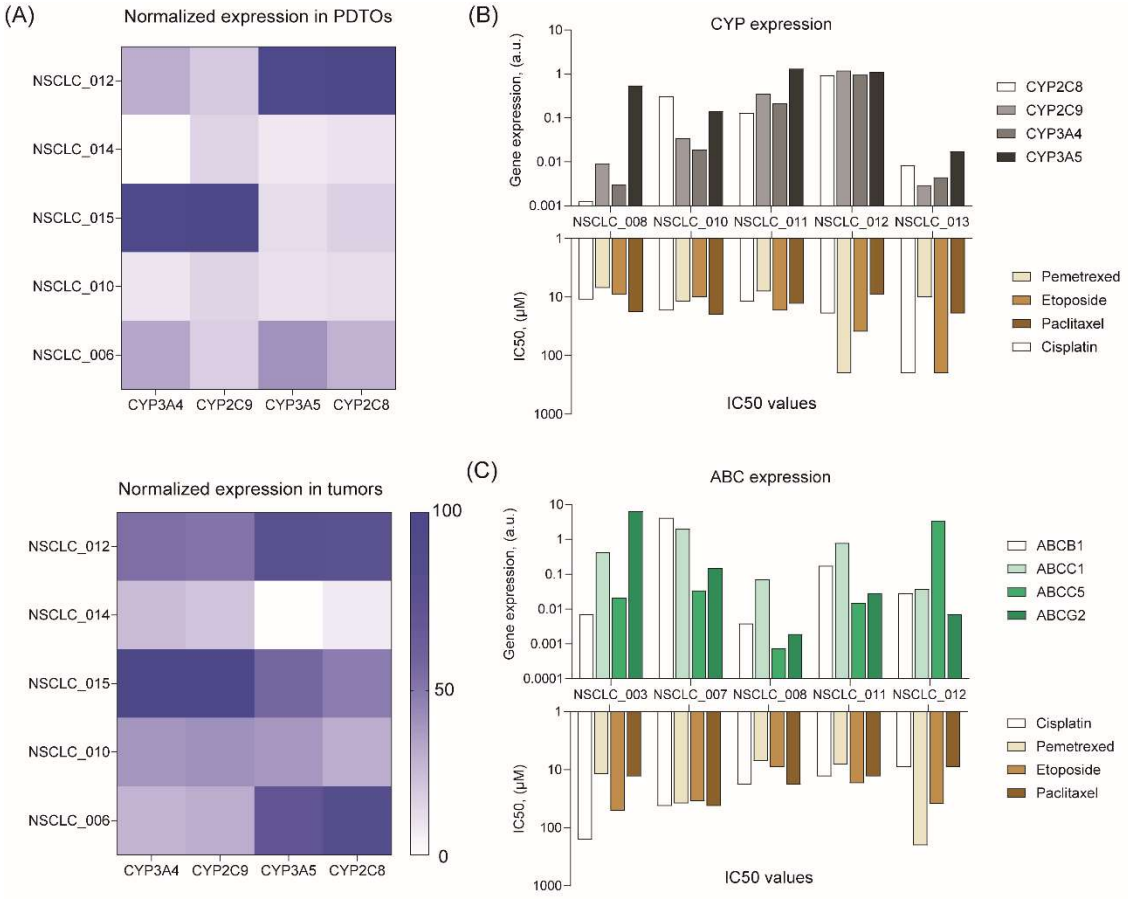

Figure 5. Analysis of drug resistance gene expression in free-floating NSCLC PDTOs. (A) Heatmaps of CYP gene expression profiles in NSCLC tumors and organoids. (B) CYP and (C) ABC gene expression levels in free-floating PDTOs versus IC50 values of chemotherapeutics.

4. DISCUSSION

PDTOs have emerged as a promising tool in personalized medicine for drug screening purposes. A few studies have demonstrated retention of the histological and genetic characteristics of the primary tumors[48] and a high prognostic value of NSCLC PDTO models.[49–52] At the same time, earlier reports mentioned the certain issues related to the production of lung cancer organoids and their properties, such as low success rate of generation,[49,53,54] fibroblast and normal epithelium overgrowth,[55] loss of immune component over time,[21] and long-term cultivation before drug testing.[49] The primary goal of this study is to generate and characterize free-floating PDTOs, obtained by a new technique (Figure 1A and B), in the light of the reported issues.

Preprints (www.preprints.org) | NOT PEER-REVIEWED | Posted: 29 December 2023 doi:10.20944/preprints202312.2280.v1

Using of stimuli-responsive ECM-mimicking gels and non-adhesive coating enables to obtain free-floating PDTOs within a one week (Figure 1C and D), while the most commonly used method of cultivation in Matrigel™ or similar ECM-like gel usually takes longer time for organoid formation.[12] Probably, the rate of intercellular contacts formation during organoid assembly plays a pivotal role in successful PDTO establishment. It has been shown that cell aggregation in tumor spheroids is mediated by E- and N-cadherins, which significantly contribute to pro-survival signaling and drug resistance.[56,57] Fast recovery of functional E-cadherin junctions is essential for survival of normal epithelial cells and cancer cells originating from highly differentiated carcinoma tumors.[58–60] Therefore, accelerated recovery of cell-cell interactions during free-floating organoid formation process could be a cause of a significant increase in establishment success rate of over 90 % (Supplemental Figure 1B) versus 40-70 % success probability for conventional NSCLC organoids.[49,52–54]

Fast assembly of free-floating organoids appears to be important not only for PDTO survival but also for better mimicking tumor microenvironment. It has been revealed that a long-term organoid cultivation often leads to overgrowth of stromal cells like cancer-associated fibroblasts,[61] or eliminating of immune cells due to lack of their expansion.[19] While the deficiency of immune cells can still be compensated for by adding them to tumor organoid culture,[62,63] solving the problem of their contamination with fibroblasts is more difficult.[54] For example, this issue could be partially resolved by a selective filtration of larger cell clusters from stromal cells before organoid establishment and modifying growth medium composition to be unfavorable for the growth of normal lung organoids.[49] As for free-floating PDTOs, they displayed expression of cancer cell-specific NSCLC markers (Figure 1F) and ECM components of connective tissues (collagen I) and basement membranes (laminin and fibronectin) (Figure 1G). Flow cytometry analysis revealed a high correlation in αSMA-positive fibroblast content between tumors and PDTOs without obvious overgrowth (Figure 2B and C). In addition, CD8+ T-cells and CD206+ positive macrophages retained in free-floating PDTOs (Figure 2B and C) in a similar percentage to the parental tumors.

Unique pattern of cytokine and growth factor expression profile in a tumor strongly affects tumor growth and development of immune tolerance. Multiple growth factors, cytokines, and their receptors are considered as significant prognostic NSCLC biomarkers.[32,64] We first evaluated whether PDTOs reproduce growth factor/cytokine expression in the parental NSCLC tumors. It turned out that expression profile in free-floating PDTOs correlated with the parental tumors in 58 % of samples (7 of 12) (Figure 3A). Significant correlations were found for six growth factor and cytokine genes, including *IL1B*, *INFG*, *EGF*, *VEGFA*, *FGF2*, and *TNFA* (Figure 3B). Thus, free-floating organoids exhibited a relatively high similarity to parental tumors in terms of morphology, cell composition, and growth factor/cytokine expression profile. Therefore, the developed organoid tumor model could be a valuable tool for personalized analysis of drug sensitivity.

In spite of increasing progress in the development of targeted therapeutics and immunotherapeutic strategies, chemotherapy remains a major first-line treatment option for advanced NSCLC in European countries so far.[7,8,65] A gold standard chemotherapy for NSCLC includes a platinum-based doublet, a combination of cisplatin (or carboplatin) with another cytostatic drug such as pemetrexed, gemcitabine, etoposide, or paclitaxel. Although tumor responsiveness to chemotherapeutics is highly variable and chemotherapy usually holds a high risk of adverse effects, there are no reliable genetic biomarkers to predict its efficacy.[5] In this context, the use of PDTOs for personalization of chemotherapy seems a promising decision.

Our data confirm a broad variation in drug sensitivity across free-floating PDTOs from different patient reaching up to two-order magnitude in IC50 value (Figure 4). IC50 values in some PDTOs exceeded C_{max} values for some drugs suggesting these PDTOs (Supplemental Figure S2) to be resistance to the certain drugs. There are several reasons for the observed variation in drug response. For example, it can be attributed to differences in expression of the genes involved in drug resistance, including cytochrome P450 (CYP) and ATP-binding cassette (ABC) transporters.[38,39,66–68] According to our data, free-floating PDTOs exhibited a high similarity in *CYP* expression with the original tumors (Figure 5A). At the same time, a high variation in *CYP* and *ABC* expression across NSCLC PDTOs

Preprints (www.preprints.org) | NOT PEER-REVIEWED | Posted: 29 December 2023 doi:10.20944/preprints202312.2280.v1

from different patients was observed (Figure 5B and C) that underscores the significance of individual drug resistance evaluation for improved therapeutic outcome. For this reason, the use of PDTOs seems very promising for personalized choice of chemotherapeutics. In addition, PDTOs can be used for evaluation of the developed ABC[69] and CYP[70] inhibitors to overcome resistance to multiple cytostatic drugs.

5. CONCLUSION

This study aimed to investigate the properties of NSCLC PDTOs obtained using free-floating method. This technique provides a high success rate of organoid establishment and accelerated assembly that enables to shorten the time between tumor tissue acquisition and drug testing up to ten days. Free-floating organoids retained similarity to the parental tumors in terms of morphology, ECM and cell composition, and cytokine/growth factor expression profile. Such characteristics make free-floating organoids a valuable tool for multiple applications including personalized drug testing.

AUTHOR CONTRIBUTIONS: The work reported in the paper has been performed by the authors, unless clearly specified in the text. Lilian Ismail: investigation, data curation, formal analysis, methodology, validation, visualization, writing – original draft. Komal Zahid: investigation, data curation, formal analysis, methodology. Anna Polyanskaya: writing – review & editing. Aya Al Othman: writing – review & editing. Shen Ningfei: writing – review & editing. Xiaoli Qi: writing – review & editing. Rushan Sulimanov: resources. Yuri Esakov: resources. Vladimir Makarov: resources, funding acquisition. Gleb Filkov: resources, project administration. Alexander Trofimenko: resources, project administration. Alexandre Mezentsev: conceptualization, data curation, formal analysis, methodology, investigation, validation, visualization, writing – original draft, writing – review & editing; Mikhail Durymanov: conceptualization, supervision, investigation, methodology, visualization, project administration, writing – original draft, writing – review & editing.

DATA AVAILABILITY STATEMENT: All relevant data are within the paper and are available to anyone for a reasonable request.

ACKNOWLEDGEMENTS: The author(s) disclosed receipt of the following financial support for the research, authorship, and/or publication of this article: This work was supported by the Ministry of Science and Higher Education of the Russian Federation within the framework of state support for the creation and development of a World-Class Research Center "Digital Biodesign and Personalized Healthcare", project # 075–15-2022–306.

CONFLICT OF INTEREST STATEMENT: The author(s) declared no potential conflicts of interest with respect to the research, authorship, and/or publication of this article.

SUPPORTING INFORMATION: Additional supporting information can be found online in the Supporting Information section at the end of this article.

References

1. Garinet S, Wang P, Mansuet-Lupo A, et al. Updated Prognostic Factors in Localized NSCLC. *Cancers* 2022; 14: 1400.
2. Leiter A, Veluswamy RR, Wisnivesky JP. The global burden of lung cancer: current status and future trends. *Nat Rev Clin Oncol* 2023; 20: 624–639.
3. Poddubskaya EV, Baranova MP, Allina DO, et al. Personalized prescription of tyrosine kinase inhibitors in unresectable metastatic cholangiocarcinoma. *Experimental Hematology & Oncology* 2018; 7: 21.
4. Poddubskaya E, Bondarenko A, Boroda A, et al. Transcriptomics-Guided Personalized Prescription of Targeted Therapeutics for Metastatic ALK-Positive Lung Cancer Case Following Recurrence on ALK Inhibitors. *Frontiers in Oncology*; 9, https://www.frontiersin.org/articles/10.3389/fonc.2019.01026 (2019, accessed 8 October 2023).
5. Szejniuk WM, Robles AI, McCulloch T, et al. Epigenetic predictive biomarkers for response or outcome to platinum-based chemotherapy in non-small cell lung cancer, current state-of-art. *Pharmacogenomics J* 2019; 19: 5–14.
6. Bepler G, Williams C, Schell MJ, et al. Randomized International Phase III Trial of ERCC1 and RRM1 Expression–Based Chemotherapy Versus Gemcitabine/Carboplatin in Advanced Non–Small-Cell Lung Cancer. *J Clin Oncol* 2013; 31: 2404–2412.

Preprints (www.preprints.org) | NOT PEER-REVIEWED | Posted: 29 December 2023 doi:10.20944/preprints202312.2280.v1

7. Lester J, Escriu C, Khan S, et al. Retrospective analysis of real-world treatment patterns and clinical outcomes in patients with advanced non-small cell lung cancer starting first-line systemic therapy in the United Kingdom. *BMC Cancer* 2021; 21: 515.
8. Bailey H, Lee A, Eccles L, et al. Treatment patterns and outcomes of patients with metastatic non-small cell lung cancer in five European countries: a real-world evidence survey. *BMC Cancer* 2023; 23: 603.
9. Olson B, Li Y, Lin Y, et al. Mouse Models for Cancer Immunotherapy Research. *Cancer Discovery* 2018; 8: 1358–1365.
10. Rozenberg JM, Filkov GI, Trofimenko AV, et al. Biomedical Applications of Non-Small Cell Lung Cancer Spheroids. *Frontiers in Oncology*; 11.
11. Lee SH, Hu W, Matulay JT, et al. Tumor Evolution and Drug Response in Patient-Derived Organoid Models of Bladder Cancer. *Cell* 2018; 173: 515-528.e17.
12. Sachs N, Papaspyropoulos A, Zomer-van Ommen DD, et al. Long-term expanding human airway organoids for disease modeling. *The EMBO Journal* 2019; 38: e100300.
13. van de Wetering M, Francies HE, Francis JM, et al. Prospective derivation of a living organoid biobank of colorectal cancer patients. *Cell* 2015; 161: 933–945.
14. Boj SF, Hwang C-I, Baker LA, et al. Organoid models of human and mouse ductal pancreatic cancer. *Cell* 2015; 160: 324–338.
15. Broutier L, Mastrogiovanni G, Verstegen MM, et al. Human primary liver cancer-derived organoid cultures for disease modeling and drug screening. *Nat Med* 2017; 23: 1424–1435.
16. Ooft SN, Weeber F, Dijkstra KK, et al. Patient-derived organoids can predict response to chemotherapy in metastatic colorectal cancer patients. *Sci Transl Med* 2019; 11: eaay2574.
17. Vlachogiannis G, Hedayat S, Vatsiou A, et al. Patient-derived organoids model treatment response of metastatic gastrointestinal cancers. *Science* 2018; 359: 920–926.
18. Francies HE, Barthorpe A, McLaren-Douglas A, et al. Drug Sensitivity Assays of Human Cancer Organoid Cultures. *Methods Mol Biol* 2019; 1576: 339–351.
19. Verduin M, Hoeben A, De Ruysscher D, et al. Patient-Derived Cancer Organoids as Predictors of Treatment Response. *Front Oncol* 2021; 11: 641980.
20. Xu H, Lyu X, Yi M, et al. Organoid technology and applications in cancer research. *J Hematol Oncol* 2018; 11: 116.
21. Neal JT, Li X, Zhu J, et al. Organoid modeling of the tumor immune microenvironment. *Cell* 2018; 175: 1972–1988.
22. Gunti S, Hoke ATK, Vu KP, et al. Organoid and Spheroid Tumor Models: Techniques and Applications. *Cancers* 2021; 13: 874.
23. Qi X, Prokhorova AV, Mezentsev AV, et al. Comparison of EMT-Related and Multi-Drug Resistant Gene Expression, Extracellular Matrix Production, and Drug Sensitivity in NSCLC Spheroids Generated by Scaffold-Free and Scaffold-Based Methods. *International Journal of Molecular Sciences* 2022; 23: 13306.
24. Durymanov MO, Rosenkranz AA, Sobolev AS. Current Approaches for Improving Intratumoral Accumulation and Distribution of Nanomedicines. *Theranostics* 2015; 5: 1007–1020.
25. Dong P, Ma L, Liu L, et al. CD86+/CD206+, Diametrically Polarized Tumor-Associated Macrophages, Predict Hepatocellular Carcinoma Patient Prognosis. *International Journal of Molecular Sciences* 2016; 17: 320.
26. Cha J-H, Chan L-C, Li C-W, et al. Mechanisms controlling PD-L1 expression in cancer. *Molecular cell* 2019; 76: 359–370.
27. Pawelczyk K, Piotrowska A, Ciesielska U, et al. Role of PD-L1 Expression in Non-Small Cell Lung Cancer and Their Prognostic Significance according to Clinicopathological Factors and Diagnostic Markers. *International Journal of Molecular Sciences* 2019; 20: 824.
28. Gennen K, Käsmann L, Taugner J, et al. Prognostic value of PD-L1 expression on tumor cells combined with CD8+ TIL density in patients with locally advanced non-small cell lung cancer treated with concurrent chemoradiotherapy. *Radiat Oncol* 2020; 15: 5.
29. Li H, Xu Y, Wan B, et al. The clinicopathological and prognostic significance of PD-L1 expression assessed by immunohistochemistry in lung cancer: a meta-analysis of 50 studies with 11,383 patients. *Transl Lung Cancer Res* 2019; 8: 429–449.
30. Ramachandran S, Verma AK, Dev K, et al. Role of Cytokines and Chemokines in NSCLC Immune Navigation and Proliferation. *Oxidative Medicine and Cellular Longevity* 2021; 2021: e5563746.
31. Bethune G, Bethune D, Ridgway N, et al. Epidermal growth factor receptor (EGFR) in lung cancer: an overview and update. *J Thorac Dis* 2010; 2: 48–51.
32. Donnem T, Andersen S, Al-Saad S, et al. Prognostic Impact of Angiogenic Markers in Non–Small-Cell Lung Cancer is Related to Tumor Size. *Clinical Lung Cancer* 2011; 12: 106–115.
33. Shibuya M. Vascular Endothelial Growth Factor (VEGF) and Its Receptor (VEGFR) Signaling in Angiogenesis: A Crucial Target for Anti- and Pro-Angiogenic Therapies. *Genes & Cancer* 2011; 2: 1097–1105.
34. Gong K, Guo G, Beckley N, et al. Tumor necrosis factor in lung cancer: Complex roles in biology and resistance to treatment. *Neoplasia* 2021; 23: 189–196.

Preprints (www.preprints.org) | NOT PEER-REVIEWED | Posted: 29 December 2023 doi:10.20944/preprints202312.2280.v1

35. Garon EB, Chih-Hsin Yang J, Dubinett SM. The Role of Interleukin 1β in the Pathogenesis of Lung Cancer. *JTO Clin Res Rep* 2020; 1: 100001.
36. Stutvoet TS, Kol A, de Vries EG, et al. MAPK pathway activity plays a key role in PD-L1 expression of lung adenocarcinoma cells. *The Journal of Pathology* 2019; 249: 52–64.
37. Liston DR, Davis M. Clinically Relevant Concentrations of Anticancer Drugs: A Guide for Nonclinical Studies. *Clinical Cancer Research* 2017; 23: 3489–3498.
38. Kaur G, Gupta SK, Singh P, et al. Drug-metabolizing enzymes: role in drug resistance in cancer. *Clin Transl Oncol* 2020; 22: 1667–1680.
39. Robey RW, Pluchino KM, Hall MD, et al. Revisiting the role of ABC transporters in multidrug-resistant cancer. *Nat Rev Cancer* 2018; 18: 452–464.
40. Sun R, Tanino R, Tong X, et al. Picropodophyllin inhibits the growth of pemetrexed-resistant malignant pleural mesothelioma via microtubule inhibition and IGF-1R-, caspase-independent pathways. *Translational Lung Cancer Research* 2022; 11: 543.
41. Sun J-M, Oh D-Y, Lee S-H, et al. The relationship between response to previous systemic treatment and the efficacy of subsequent pemetrexed therapy in advanced non-small cell lung cancer. *Lung Cancer* 2010; 68: 427–432.
42. Chen J, Wang Z, Gao S, et al. Human drug efflux transporter ABCC5 confers acquired resistance to pemetrexed in breast cancer. *Cancer Cell Int* 2021; 21: 136.
43. Chen B, Zhang D, Kuai J, et al. Upregulation of miR-199a/b contributes to cisplatin resistance via Wnt/β-catenin-ABCG2 signaling pathway in ALDHA1+ colorectal cancer stem cells. *Tumor Biology* 2017; 39: 1010428317715155.
44. Niu Q, Wang W, Li Y, et al. Low molecular weight heparin ablates lung cancer cisplatin-resistance by inducing proteasome-mediated ABCG2 protein degradation. *PLoS One* 2012; 7: e41035.
45. Su J, Wu S, Tang W, et al. Reduced SLC27A2 induces cisplatin resistance in lung cancer stem cells by negatively regulating Bmi1-ABCG2 signaling. *Molecular carcinogenesis* 2016; 55: 1822–1832.
46. Yin X, Liao Y, Xiong W, et al. Hypoxia-induced lncRNA ANRIL promotes cisplatin resistance in retinoblastoma cells through regulating ABCG2 expression. *Clinical and Experimental Pharmacology and Physiology* 2020; 47: 1049–1057.
47. Zhang W, Yu F, Wang Y, et al. Rab23 promotes the cisplatin resistance of ovarian cancer via the Shh-Gli-ABCG2 signaling pathway. *Oncology letters* 2018; 15: 5155–5160.
48. Chen J-H, Chu X-P, Zhang J-T, et al. Genomic characteristics and drug screening among organoids derived from non-small cell lung cancer patients. *Thorac Cancer* 2020; 11: 2279–2290.
49. Hu Y, Sui X, Song F, et al. Lung cancer organoids analyzed on microwell arrays predict drug responses of patients within a week. *Nat Commun* 2021; 12: 2581.
50. Koga T, Soh J, Hamada A, et al. Clinical Relevance of Patient-Derived Organoid of Surgically Resected Lung Cancer as an In Vitro Model for Biomarker and Drug Testing. *JTO Clin Res Rep* 2023; 4: 100554.
51. Kim S-Y, Kim S-M, Lim S, et al. Modeling Clinical Responses to Targeted Therapies by Patient-Derived Organoids of Advanced Lung Adenocarcinoma. *Clin Cancer Res* 2021; 27: 4397–4409.
52. Wang H-M, Zhang C-Y, Peng K-C, et al. Using patient-derived organoids to predict locally advanced or metastatic lung cancer tumor response: A real-world study. *Cell Rep Med* 2023; 4: 100911.
53. Della Corte CM, Barra G, Ciaramella V, et al. Antitumor activity of dual blockade of PD-L1 and MEK in NSCLC patients derived three-dimensional spheroid cultures. *Journal of Experimental & Clinical Cancer Research* 2019; 38: 253.
54. Dijkstra KK, Monkhorst K, Schipper LJ, et al. Challenges in Establishing Pure Lung Cancer Organoids Limit Their Utility for Personalized Medicine. *Cell Rep* 2020; 31: 107588.
55. Si L-L, Lv L, Zhou W-H, et al. Establishment and identification of human primary lung cancer cell culture in vitro. *Int J Clin Exp Pathol* 2015; 8: 6540–6546.
56. Huang Y-J, Hsu S. Acquisition of epithelial–mesenchymal transition and cancer stem-like phenotypes within chitosan-hyaluronan membrane-derived 3D tumor spheroids. *Biomaterials* 2014; 35: 10070–10079.
57. Lin R-Z, Chou L-F, Chien C-CM, et al. Dynamic analysis of hepatoma spheroid formation: roles of E-cadherin and beta1-integrin. *Cell Tissue Res* 2006; 324: 411–422.
58. Kantak SS, Kramer RH. E-cadherin Regulates Anchorage-independent Growth and Survival in Oral Squamous Cell Carcinoma Cells *. *Journal of Biological Chemistry* 1998; 273: 16953–16961.
59. Goncharova EA, Goncharov DA, James ML, et al. Folliculin controls lung alveolar enlargement and epithelial cell survival through E-cadherin, LKB1, and AMPK. *Cell reports* 2014; 7: 412–423.
60. Manuel Iglesias J, Beloqui I, Garcia-Garcia F, et al. Mammosphere formation in breast carcinoma cell lines depends upon expression of E-cadherin. *PloS one* 2013; 8: e77281.
61. Ko YR, Kim JM, Kang Y, et al. A method for culturing patient-derived lung cancer organoids from surgically resected tissues and biopsy samples. *Organoid*; 2. Epub ahead of print 25 July 2022. DOI: 10.51335/organoid.2022.2.e19.

Preprints (www.preprints.org) | NOT PEER-REVIEWED | Posted: 29 December 2023 doi:10.20944/preprints202312.2280.v1

62. Dijkstra KK, Cattaneo CM, Weeber F, et al. Generation of Tumor-Reactive T Cells by Co-culture of Peripheral Blood Lymphocytes and Tumor Organoids. *Cell* 2018; 174: 1586-1598.e12.
63. Valančiūtė A, Mathieson L, O'Connor RA, et al. Phototherapeutic Induction of Immunogenic Cell Death and CD8+ T Cell-Granzyme B Mediated Cytolysis in Human Lung Cancer Cells and Organoids. *Cancers (Basel)* 2022; 14: 4119.
64. Silva EM, Mariano VS, Pastrez PRA, et al. High systemic IL-6 is associated with worse prognosis in patients with non-small cell lung cancer. *PLOS ONE* 2017; 12: e0181125.
65. Pirker R. Chemotherapy remains a cornerstone in the treatment of nonsmall cell lung cancer. *Current Opinion in Oncology* 2020; 32: 63.
66. Zhao M, Ma J, Li M, et al. Cytochrome P450 Enzymes and Drug Metabolism in Humans. *International Journal of Molecular Sciences* 2021; 22: 12808.
67. Fletcher JI, Williams RT, Henderson MJ, et al. ABC transporters as mediators of drug resistance and contributors to cancer cell biology. *Drug Resistance Updates* 2016; 26: 1–9.
68. Zhou S-F, Wang L-L, Di YM, et al. Substrates and inhibitors of human multidrug resistance associated proteins and the implications in drug development. *Current medicinal chemistry* 2008; 15: 1981–2039.
69. Budagaga Y, Sabet Z, Zhang Y, et al. Tazemetostat synergistically combats multidrug resistance by the unique triple inhibition of ABCB1, ABCC1, and ABCG2 efflux transporters in vitro and ex vivo. *Biochemical Pharmacology* 2023; 216: 115769.
70. Zhou L, Chen W, Cao C, et al. Design and synthesis of α-naphthoflavone chimera derivatives able to eliminate cytochrome P450 (CYP)1B1-mediated drug resistance via targeted CYP1B1 degradation. *European Journal of Medicinal Chemistry* 2020; 189: 112028.

Disclaimer/Publisher's Note: The statements, opinions and data contained in all publications are solely those of the individual author(s) and contributor(s) and not of MDPI and/or the editor(s). MDPI and/or the editor(s) disclaim responsibility for any injury to people or property resulting from any ideas, methods, instructions or products referred to in the content.